Journal of Controlled Release 394 (2026) 114867

Contents lists available at ScienceDirect

Journal of Controlled Release

journal homepage: www.elsevier.com/locate/jconrel

Injectable and transient hydrogel with programmable lifetime by endogenous coordination crosslinking and enzymatic de-crosslinking☆

Ryo Sekiya [a], Masahiko Nakamoto [a,b,*], Shunsuke Kato [a,c,d], Takashi Hayashi [a], Michiya Matsusaki [a,*]

[a] Division of Applied Chemistry, Graduate School of Engineering, The University of Osaka, 2-1 Yamada-oka, Suita, Osaka 565-0871, Japan
[b] Center for Future Innovation (CFi), Faculty of Engineering, The University of Osaka, 2-1 Yamada-oka, Suita, Osaka 565-0871, Japan
[c] Graduate School of Science, Technology, and Innovation, Kobe University, 1-1 Rokkodai, Nada, Kobe, 657-8501, Japan
[d] Engineering Biology Research Center, Kobe University, 1-1 Rokkodai, Nada, Kobe 657-8501, Japan

ABSTRACT

We developed an injectable and transient hydrogel with a programmable lifetime by introducing closed functional loops, specifically gelation and sol transition pathways, within the system. Gelation occurs through the formation of coordination crosslinking between a phosphate ester and its affinity ligand, while enzymatic degradation of the phosphate ester triggers the sol transition pathway. The transition from the gel to the sol state was driven by the dissipation of a transient thermodynamic state under out-of-equilibrium conditions. The transient gel persisted because of the kinetic imbalance between fast gelation and the slow sol transition pathway. By tuning the kinetic balance of these pathways, the lifetime of the transient hydrogel was programmed over a wide range—from within an hour to three months. Additionally, the ability of the hydrogel to control the payload release induced by sol transition was validated. The unique properties of the present system are expected to have applications in drug delivery systems tailored to patient needs and objectives, as well as in scaffold materials for tissue engineering.

1. Introduction

Hydrogels have been developed in the biomedical field for applications such as drug delivery, wound dressings, and scaffolds for tissue engineering owing to their biocompatibility, softness, porous structure, and excellent swelling properties [1,2]. Among them, injectable hydrogels, typically formed through in situ chemical and/or physical crosslinking, have attracted significant attention because they can be locally administered to the target site by simple manipulation without surgery, thereby overcoming side effects and poor drug distribution and improving therapeutic intervention [3]. Tetra-branched polyethylene glycols (tetra-PEGs) have a tetrahedral structure and thus form a uniform hydrogel by crosslinking at their termini [4]. Tetra-PEG gels with a homogeneous network structure were developed using two tetra-PEG with either activated carboxylate esters or amine groups as precursors [5–7]. Non-covalently crosslinkages [8–13], such as avidin-biotin interactions [8] and DNA hybridization [11], have also been employed in fabricating tetra-PEG-based hydrogels. The gel-to-sol transition of injectable gels is effective for enhancing payload release and/or facilitating cell proliferation and migration [14]. Thus, to control the sol transition behavior of injectable gels, systems containing crosslinked structures that degrade in response to various stimuli, such as enzymes, pH, and/or temperature, have been widely studied [15]. In general, the sol transition of these gels is controlled by changes in the thermodynamic equilibrium state upon the addition of stimuli.

In contrast, many biological processes form kinetically regulated closed functional loops rather than being in equilibrium. For example, kinetically controlled phosphorylation/dephosphorylation by kinases/phosphatases regulates several biological functions. Smooth muscle contraction is regulated by the reversible phosphorylation of actin and myosin filaments [16]. Phosphorylation of certain proteins promotes the timely degradation of polyubiquitinated proteins via selective autophagy [17]. Such a dynamic nature enables unique biological properties, including a tunable lifetime and structural and functional complexities. In this context, hydrogels that function under out-of-equilibrium conditions as living systems have been developed [18]. J. Boekhoven et al. reported the transient gelation of synthetic molecules by engineering a chemically fueled reaction network involving the activation and deactivation of building blocks [19,20]. Poly(*N*-isopropylacrylamide)-based polymers/hydrogels functionalized with a catalyst for the

☆ This article is part of a Special issue entitled: 'Young Investigator Issue' published in Journal of Controlled Release.

* Corresponding authors at: Division of Applied Chemistry, Graduate School of Engineering, The University of Osaka, 2-1 Yamada-oka, Suita, Osaka 565-0871, Japan.

E-mail address: m-nakamoto@chem.eng.osaka-u.ac.jp (M. Nakamoto).

https://doi.org/10.1016/j.jconrel.2026.114867
Received 27 March 2025; Received in revised form 20 March 2026; Accepted 24 March 2026
Available online 25 March 2026

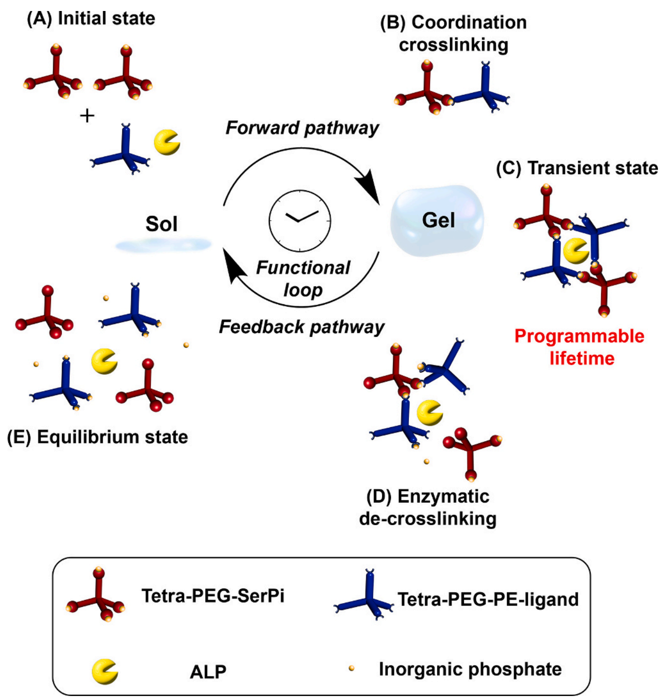

Fig. 1. Conceptual illustration of this study. (A) As hydrogel precursors, tetra-branched polyethylene glycols (tetra-PEGs) with either a phosphate ester (tetra-PEG-SerPi) or an affinity ligand of phosphate ester (tetra-PEG-PE-ligand) were prepared. Prior to mixing two precursors, alkaline phosphatase (ALP) was encapsulated into the tetra-PEG-PE-ligand. (B) Crosslinked structure by coordination between SerPi and PE-ligand is rapidly formed upon mixing two tetra-PEG precursors as the forward pathway. (C) Obtained hydrogel persists transiently. (D) The transient state is dissipated through slow enzymatic de-crosslinking catalyzed by encapsulated ALP as an internal feedback pathway. (E) At the end of the loop, the gel automatically turns into a solution state at thermodynamic equilibrium.

Belousov–Zhabotinsky (BZ) reaction have demonstrated oscillatory structural changes [21–23]. A hydrogel film consisting of thiol-terminated tetra-PEG and crosslinkers facilitated electricity-powered temporal modulation of hydrogel stiffness through the formation of transient cross-links [24]. Functions under extreme or limited conditions differ significantly from those under normal biological conditions, and the use of biomolecules as fuel and/or catalysts for functions far from equilibrium is of great interest for their application in biomaterials. For example, supramolecular self-assembly fueled by ATP, peptide derivatives, and DNA has been demonstrated in enzyme-catalyzed reaction networks [25–30]. Hydrogels with affinity and digestive capacity for biomacromolecules exhibit transient volume phase transitions [31,32]. H. Jo et al. reported a system comprised of *Staphylococcus epidermidis* and telechelic block copolymers exhibited transient and macroscopic phase transition fueled by D-glucose [33].

Inspired by kinetically controlled signal transduction through phosphorylation/dephosphorylation, we report an injectable and transient gel system with an endogenous pathway for sol transition (Fig. 1). The system comprises a closed functional loop. Mixing two tetra-PEGs with either a phosphate ester (tetra-PEG-SerPi) or an affinity ligand of phosphate ester; an alkoxide-bridged dinuclear zinc(II) complex, which recognize phosphate monoester dianion in an aqueous solution at a neutral pH [34–36]. (tetra-PEG-PE-ligand) forms a crosslinked structure by coordination, which induces gelation. In parallel, encapsulated alkaline phosphatase (ALP) catalyzes de-crosslinking as a dissipative process. Because of the kinetic imbalance between these forward and feedback pathways, the gel persists as a temporarily stable gel state (transient gel), followed by an autonomous, programmable, and external stimulus-free sol transition. By controlling the kinetic balance of the two pathways, the lifetime of the hydrogel can be programmed over a wide range (from hours to months). Additionally, the capability of the hydrogel to control payload release is demonstrated. Our study provides a foundation for engineering injectable hydrogels with programmable functional lifetimes that operate far from equilibrium, enabling their use as carriers for drugs, proteins, and/or cells in drug release systems and/or tissue engineering.

1.1. Materials and instrumentation

Pentaerythritoltetra(succinimidylcarboxypentyl)polyoxyethylene (tetra-PEG-NHS) (MW = 20 kDa) was purchased from the NOF CORPORATION (TY, Japan). *O*-Phospho-L-serine (SerPi), zinc chloride, disodium *p*-nitrophenyl phosphate hexahydrate, and fluorescein diphosphate tetraammonium salt (FDP) were purchased from FUJIFILM Wako Pure Chemical Corporation (OS, Japan). The amino-pendant Phos-tag™ ligand was purchased from the Nard Institute Ltd. (HG, Japan). Alkaline phosphatase (ALP) (from bovine intestinal mucosa) were purchased from Sigma-Aldrich Co. (MO, USA). Dulbecco's modified eagle medium (DMEM) (high glucose and phosphate free) and a LIVE/DEAD™ viability/cytotoxicity kit for mammalian cells were purchased from Thermo Fisher Scientific (MA, USA). The human breast cancer cell line (MDA-MB-231) was obtained from KAC Co. Ltd. (KY, Japan). Ultra violet-visible (UV–Vis) absorption spectra were measured using a NanoDropTM 2000c (Thermo Fisher Scientific, MA, USA) or UV–Visible spectrophotometer (V-670; JASCO, TY, Japan) for polymer characterization or enzymatic assays. Lyophilization of the polymer samples was performed using an FDU-2200 lyophilizer (EYELA, TY, Japan). ^{1}H nuclear magnetic resonance (^{1}H NMR) spectrum of the obtained polymers were acquired using a 400-MHz NMR spectrometer (JEOL, TY, Japan). The rheologies of the hydrogel formulations were determined using a modular compact rheometer (MCR302; Anton Paar, OS, Japan). A UV lamp (AS ONE, Osaka, Japan) was used to visualize the enzymatic reactions during the sol transition. Fluorescence spectra were recorded using an FP-8500 spectrofluorometer (JASCO, TY, Japan). Confocal images were obtained using Cell Voyager CQ1 (Yokogawa Electric Corporation, TY, Japan).

2. Experiments

2.1. Synthesis of Tetra-PEG-SerPi

Briefly, 44 mg of SerPi (240 μmol, 48.0 eq.) was dissolved in 4 mL of a 4-(2-hydroxyethyl)-1-piperazineethanesulfonic acid (HEPES) buffer (500 mM, pH 7.4), followed by the addition of 100 mg of tetra-PEG-NHS (5.0 μmol, 1.0 eq.). The solution was incubated at 37 °C for 24 h in a rotary shaker. Subsequently, the solution was dialyzed against water for two days using a dialysis membrane with a cut-off of 3.5 kDa. Finally, purified tetra-PEG-SerPi was obtained by lyophilization for three days. The amount of SerPi in tetra-PEG was determined by ^{1}H NMR spectrometry at 400 MHz (5 g L^{-1} in D_2O) (JEOL, TY, Japan).

2.2. Synthesis of Tetra-PEG-PE-ligand

5.5 μL triethylamine (TEA) (40 μmol, 8.0 eq.) and 22 mg of Phos-tag (40 μmol, 8.0 eq.) were dissolved in 4.0 mL of tetrahydrofuran (THF), followed by the addition of 100 mg of tetra-PEG-NHS (5.0 μmol, 1.0 eq.). The solution was incubated at 37 °C for 24 h in a rotary shaker. Subsequently, the solution was diluted five-fold using water and dialyzed against 5 mM $ZnCl_2$aq for one day and water for one day using a dialysis membrane with a cut-off of 3.5 kDa. Finally, the purified tetra-PEG-PE-ligand was obtained by lyophilization for three days. The amount of the PE-ligand in tetra-PEG and coordination of zinc ions to the PE-ligand were determined using ^{1}H NMR spectrometry at 400 MHz (5 g L^{-1} in D_2O). The introduction of the PE-ligand was also confirmed by UV absorption at 260 nm.

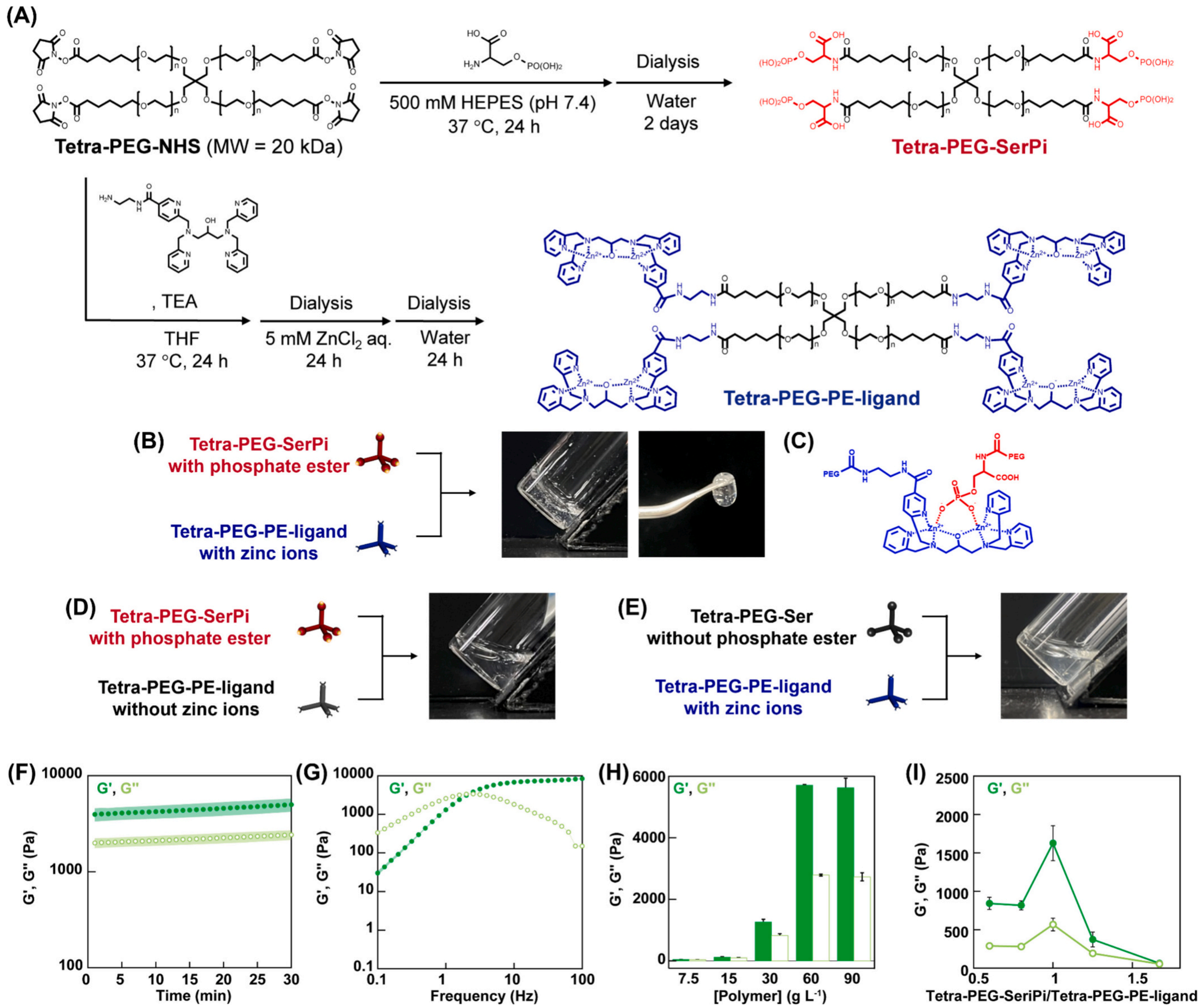

Fig. 2. (A) Synthesis scheme of tetra-PEG-SerPi and tetra-PEG-PE-ligand. (B) Gelation upon mixing tetra-PEG-SerPi and tetra-PEG-PE-ligand. (C) Chemical structure of coordination crosslinking. Lack of gelation upon mixing (D) tetra-PEG-SerPi and tetra-PEG-PE-ligand without zinc ions / (E) tetra-PEG-Ser without phosphate esters and tetra-PEG-PE-ligand. (F) Time courses of G' and G" during gelation after mixing the two gel precursors. (G) G' and G" of the hydrogel in frequency sweep measurements. (H) G' and G" of the hydrogel under various polymer concentrations. The weight ratio of polymers was fixed at 1: 1 (f = 5 Hz). (I) Dependence of G' and G" on the stoichiometric ratio of two polymers (f = 5 Hz). (B), (D)–(G) and (I) Total polymer concentration was fixed at 30 g L^{-1}. (F)–(I) G' and G" are shown as closed green and open light green, respectively, with the shaded area or error bars representing SD ($n = 3$). Some errors are small and not visible. (For interpretation of the references to colour in this figure legend, the reader is referred to the web version of this article.)

2.3. Preparation of injectable hydrogel

Each precursor was dissolved in the HEPES buffer (100 mM, pH 7.4) at the same concentration. The discrimination between the gel and sol states was determined by whether the surface of the solution or hydrogel was parallel to the bottom of the screw tube when the screw tube was tilted at respective time. For cell culture, the hydrogels were prepared in the same manner, except for the use of DMEM (without phosphates, with 50 mM HEPES) supplemented with 10% fetal bovine serum (FBS) and 1% antibiotics as solvents.

2.4. Preparation of injectable and transient hydrogel

First, 1 μL of an ALP solution (0.001 to 10 unit) was added to 100 μL of a tetra-PEG-PE-ligand precursor solution. This solution was mixed with 100 μL of a tetra-PEG-SerPi precursor solution. The enzymatic reaction during sol transition was visualized using a hydrogel encapsulating both ALP (0.1 unit) and FDP (250 μM). The hydrogel was kept at 25 °C, in a dark room, and observed over time under 365-nm UV light. The fluorescence intensity of the FDP at each timepoint was quantified via fluorescence measurements. The excitation and emission wavelengths were 490 and 521 nm, respectively.

2.5. Rheology measurement

The rheology of the hydrogel was investigated by oscillatory time-sweep measurements at a strain of 0.5% and a constant frequency of 5 Hz using a rheometer with a 25-mm parallel plate. After mixing the precursors, 600 μL of hydrogel was immediately placed in the rheometer, and its storage modulus (G') and loss modulus (G") were recorded at 10-s intervals. In frequency sweep measurements, G' and G" were recorded as functions of shear frequency in the range 0.1–100 Hz at a

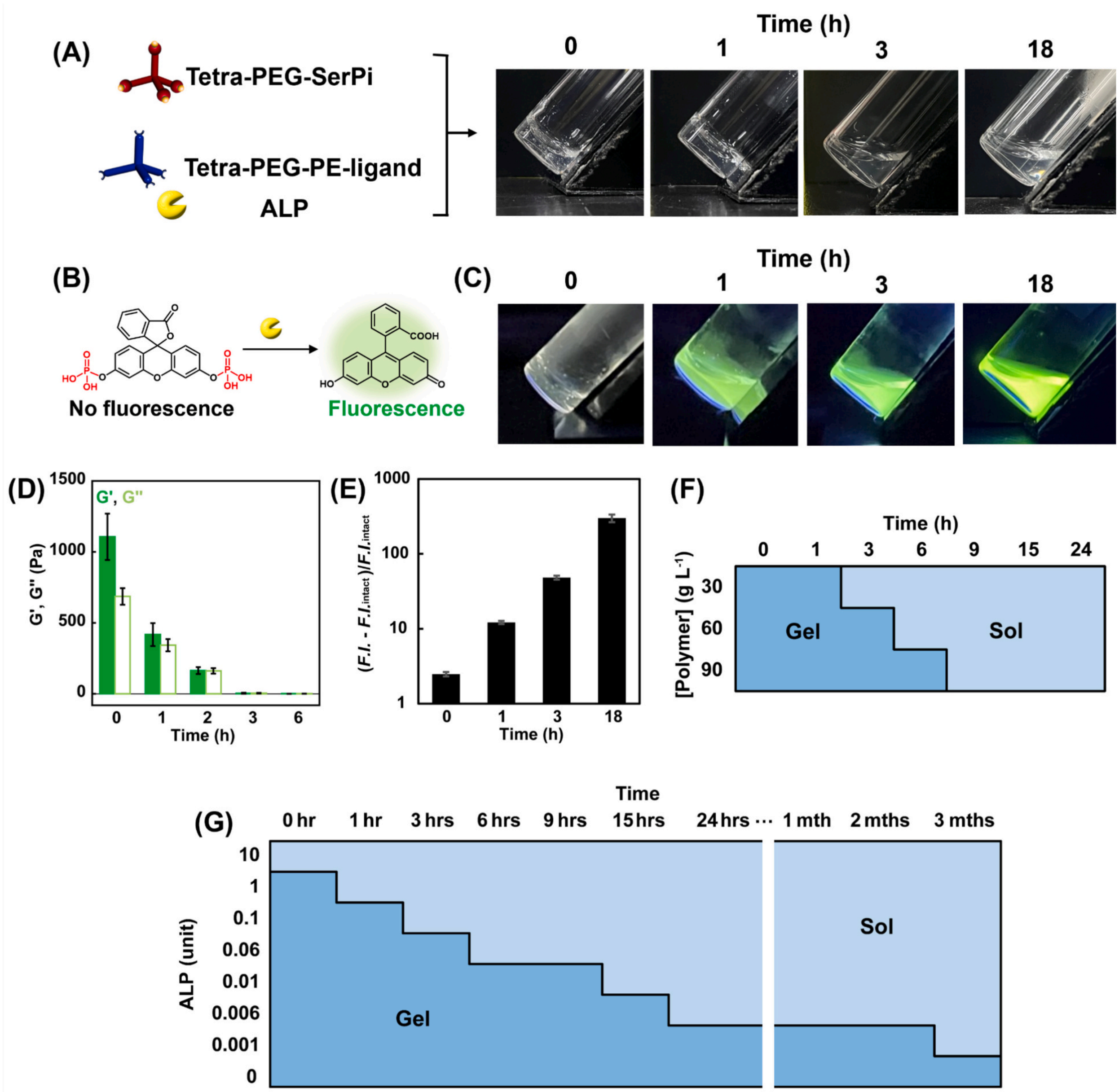

Fig. 3. (A) Photographs of transient gel and its sol transition. (B) Chemical structure of phosphatase-responsive fluorophore: FDP. (C) Photographs of transient gel and its sol transition in the presence of FDP in gel. (D) G' and G" of transient gel on the sol transition. G' and G" are shown as closed green and open light green squares, respectively ($n = 3$). (E) Fluorescence intensity of FDP within transient hydrogel (n = 3). Programing the lifetime of the transient gels by tuning (F) polymer concentration and (G) ALP concentration. (For interpretation of the references to colour in this figure legend, the reader is referred to the web version of this article.)

fixed strain of 0.5%. A 600 μL aliquot of the hydrogel was loaded onto the rheometer 20 min after mixing. All measurements were carried out at 37 °C; moistened cotton was deposited around the sample to prevent evaporation.

2.6. Programmed release of payload

100 μL of a tetra-PEG-SerPi precursor solution (30 g L^{-1}) containing ALP (0.1 or 1 unit) and 100 μM FDP was mixed with 100 μL of the tetra-PEG-PE-ligand precursor solution (30 g L^{-1}) in a micro tube to prepare a hydrogel with 50 μM FDP. 800 μL of the HEPES buffer (100 mM, pH 7.4) was added on top of the gel, and the tube was maintained at 37 °C. The release of payload was quantified based on the fluorescence intensity of the supernatant. The excitation and emission wavelengths were 490 and 521 nm, respectively. Prior to the measurement, 1 μL of ALP (10 g L^{-1}) was added to 10 μL of the collected supernatant and kept at 37 °C for 3 h to eliminate phosphate ester completely. For the programmed release of a phosphate ester-tagged protein, 0.5 μM enhanced green fluorescein protein with phosphate ester tag (EGFP-Pi) was encapsulated in a gel, and its release was quantified based on the fluorescence intensity of the supernatant. The excitation and emission wavelengths were 488 and 509 nm, respectively.

2.7. Biocompatibility

To investigate the biocompatibility of this material, the survival of cells with the hydrogel was assessed using a live–dead assay. In brief, 100 μL of the hydrogel was prepared on MDA-MB-231 cells (5.0×10^3 cells/well) in a DMEM buffer (without phosphates, with 50 mM HEPES) supplemented with 10% FBS and 1% antibiotics in 96 well plates. The cells were incubated for 24 h at 37 °C and 5% CO_2. For the live–dead assay, solution A was prepared by adding 1 μL of calcein-acetoxymethylester (calcein-AM) and 4 μL of ethdium homodeimer-1 to 200 μL of Dulbecco's phosphate-buffered saline (D-PBS). Solution A was added at 10 μL/well on each hydrogel and incubated for 1 h at 37 °C, 5% CO_2. Subsequently, we observed the cells using confocal scanning laser microscopy.

3. Results and discussion

3.1. Gelation by coordination crosslinking between precursors

Two four-arm poly-ethylene glycol (tetra-PEG) derivatives, functionalized with either phosphorylated amino acids (SerPi) or affinity ligands of phosphate esters (PE-ligand) at their termini, were prepared as gel precursors (Fig. 2A). The degrees of introduction of SerPi and the PE-ligand were determined to be 87% and 91%, respectively, via ^{1}H NMR (Fig. S1). The coordination of zinc ions to the PE-ligand were also confirmed via ^{1}H NMR. UV absorption from the PE-ligand group quantified the degree of introduction as 106% (Fig. S2). Two precursor solutions were prepared by dissolving tetra-PEG-SerPi (30 g L^{-1}) or tetra-PEG-PE-ligand (30 g L^{-1}) in the HEPES buffer (100 mM, pH 7.4). A transparent hydrogel was immediately obtained by mixing equal volumes of the two gel precursors (total volume: 200 μL) (Fig. 2B), which suggest the formation of coordination crosslinkages (Fig. 2C). In contrast, no gelation was observed when a tetra-PEG-PE-ligand without zinc ions or a tetra-PEG-Ser without phosphate esters was used as a precursor (Fig. 2D and E). These results indicate that coordination crosslinking between the PE-ligand and SerPi is the driving force for gelation.

Rheological measurements showed that gelation proceeded within a few tens of seconds (Fig. 2F). The storage modulus (G') was higher than the loss modulus (G") in the high-frequency region with a crossover frequency observed around 2 Hz (Fig. 2G). Such frequency-dependent viscoelastic behavior, characterized by the presence of a crossover between G′ and G″, is a typical feature of physically crosslinked hydrogels with reversible crosslinking, in contrast to chemically crosslinked hydrogels, which generally exhibit frequency-independent moduli.

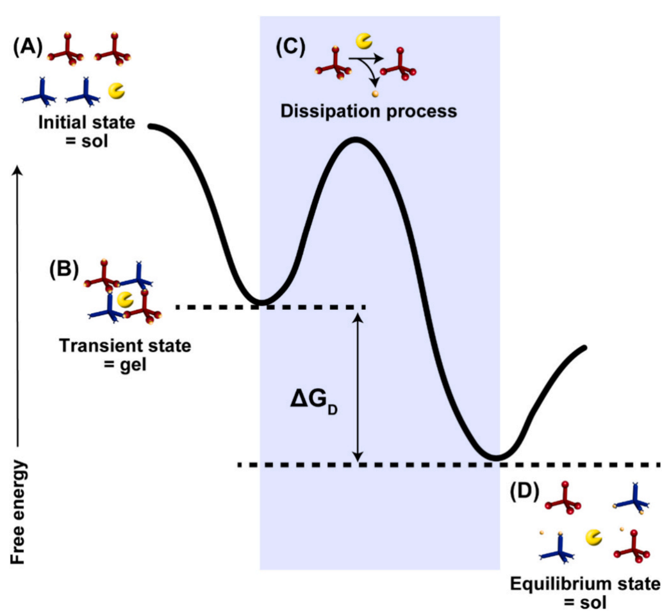

Fig. 4. Qualitative energy landscape of the transient hydrogel system. (A) Mixing two tetra-PEG precursors in the presence of ALP leads to (B) a transient state, in which the polymers form a hydrogel network via rapid coordination crosslinking. (C) This kinetically trapped state is gradually dissipated through slow enzymatic dephosphorylation, which facilitates the sol transition. (D) Ultimately, the gel autonomously transitions into the solution state at thermodynamic equilibrium.

These results indicate the presence of non-covalent and reversible crosslinkages within the hydrogel network [37,38]. The obtained hydrogel was also characterized by scanning electron microscopy (SEM), revealing a morphology similar to that reported earlier (Fig. S3) [39,40].

Hydrogels were formed when the polymer concentration exceeded 30 g L^{-1} and G' increased from 1.3 kPa to 5.7 kPa with an increase in the polymer concentration from 30 g L^{-1} to 60 g L^{-1}, indicating the formation of a denser hydrogel network (Figs. 2H and S4). The concentration-dependent increase in G′ supports the formation of a more robust hydrogel network. As the concentration increases, the sol-gel equilibrium shifts toward gel formation, resulting in a greater contribution of G' relative to G". In contrast, both G' and G" changed slightly upon further increasing the polymer concentration from 60 g L^{-1} to 90 g L^{-1}, indicating that the network was already fully developed. When the polymer concentration was lower than 15 g L^{-1}, the weaker network led to a marked decrease in modulus, indicating a viscous liquid rather than a hydrogel. The effect of the stoichiometric ratio of the two precursors on the mechanical properties was further investigated (Fig. 2I). The hydrogel showed the highest G' when at a stoichiometric ratio of 1:1, which indicates that a homogeneous network without defects provides the stiffness of a gel. We also observed that G' was higher than G" within the range of 10 to 40 °C by temperature sweep measurements (Fig. S5). In summary, two tetra-PEGs functionalized with either SerPi or PE-ligand formed a tetra-PEG gel with measurable rheological properties via phosphate ester-mediated coordination crosslinking.

3.2. Transient hydrogel with programmable lifetime

An injectable gel system with a closed functional loop, consisting of two pathways: a rapid gelation via coordination crosslinking and a slower sol transition facilitated by enzymatic dephosphorylation, is expected to exhibit transient gelation with a finite lifetime. Before validating this hypothesis, we first confirmed that ALP catalyzes dephosphorylation of tetra-PEG-SerPi (Supporting Information 5 and 6), indicating that ALP can function as a de-crosslinking pathway in the system. Based on these results, we developed a transient gel system by encapsulating ALP in a tetra-PEG-PE-ligand precursor prior to mixing. Rapid gelation was observed upon mixing the two precursors within several tens of seconds. This gel state persisted for approximately 1 h, after which it autonomously transitioned into a solution state within 3 h (Fig. 3A). Furthermore, to visualize the dephosphorylation process, FDP, a fluorogenic substrate that releases fluorescein upon dephosphorylation catalyzed by ALP, was encapsulated within the transient gel system. As a result, fluorescence growth was observed to coincide with the autonomous sol transition, indicating that the ALP-catalyzed de-crosslinking pathway facilitates the sol transition (Fig. 3B and C). Rheological measurements over time showed a decrease in modulus and loss of hydrogel properties (Figs. 3D and S11). In addition, the time scale of fluorescence growth derived from enzymatic hydrolysis of FDP during the sol transition of the FDP-loaded system was clearly slower than the gelation process (Fig. 3E). Thus, this transient gelation was achieved through a kinetic imbalance between the fast gelation pathway and the slow sol transition pathway under given condition. This interpretation is also supported by the kinetic analysis of in-gel enzymatic dephosphorylation (Supporting Information 7 and 8). We first confirmed that the addition of the same amount of ALPs to the pre-formed gel required a longer time for the sol transition (Fig. S8). In addition, comparable enzymatic reaction kinetics of in-gel ALP and free ALP were observed (Fig. S9 and S10). These results indicate that ALP could be distributed and act homogeneously in the transient gel system. Accordingly, tuning the kinetic balance between these two pathways would enable control over the lifetime of the gel.

Thus, we investigated the changes in the hydrogel lifetime with variations in the concentrations of polymers/ALPs (Fig. 3F and G). At a fixed ALP concentration (0.1 unit), the hydrogel lifetime increased with

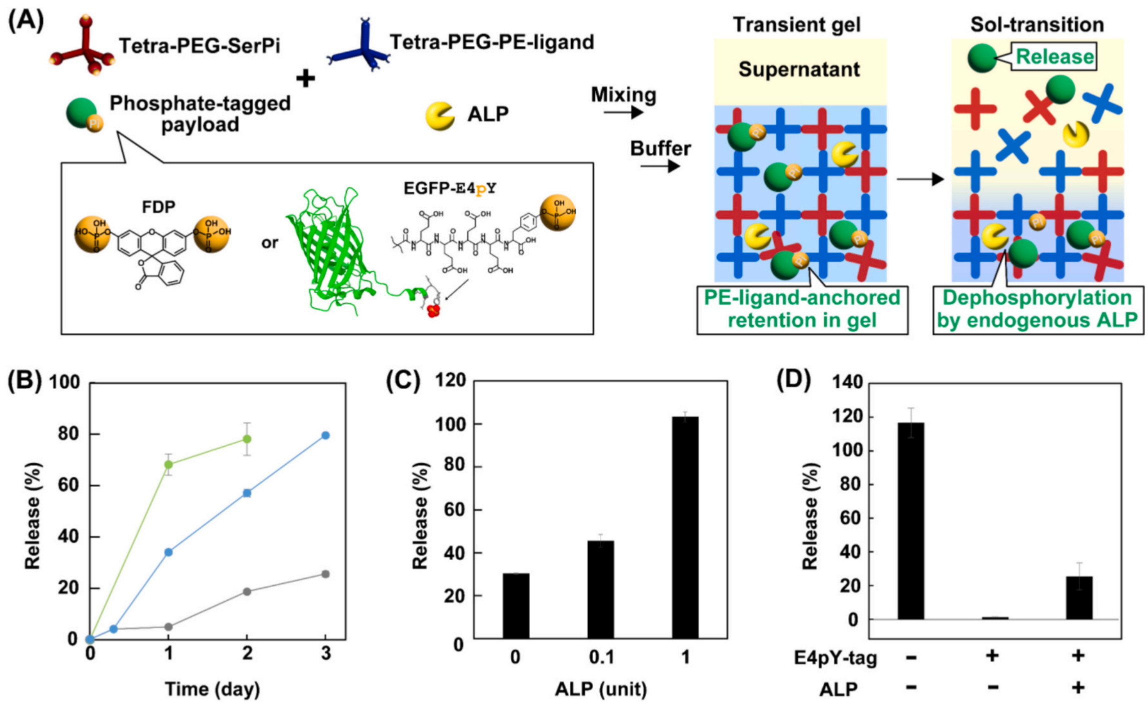

Fig. 5. (A) Schematic illustration of programmed retention and release of phosphate ester-tagged payload. (B) Release of FDP with phosphate esters (gray) and fluorescein without phosphate ester (green) from the gel without ALP. Controlled release of FDP from the gel with ALP encapsulation (blue). (C) Release of FDP from the gel with varied amounts of ALP at six days. (D) Release of EGFPs with/without E4pY-tag from the gel with/without ALP (1 unit) at six days. (B), (C), and (D) n = 3. (For interpretation of the references to colour in this figure legend, the reader is referred to the web version of this article.)

increasing polymer concentration (Fig. 3F). Higher polymer concentrations result in a denser hydrogel network. Such network densification suppresses network collapse and the subsequent sol transition, as a higher degree of de-crosslinking is required to disrupt the hydrogel network. As a result, increasing the polymer concentration prolongs the lifetime of the hydrogel.

Subsequently, we investigated the changes in the hydrogel lifetime with variations in the concentrations of encapsulated ALPs at a fixed polymer concentration (30 g L^{-1}). The results showed that the hydrogel lifetime decreased with increasing ALP concentration (Fig. 3G). It is considered that a higher concentration of encapsulated enzymes promotes dephosphorylation and accelerates the sol transition. The relationship between ALP concentration and hydrogel lifetime exhibited an exponential trend (Fig. S12). We also observed the gradual decay of ALP activity over time (Fig. S13). These observations suggest that the time-dependent decay of enzymatic activity also contributes to the lifetime of the transient hydrogel in addition to the enzymatic hydrolysis kinetics, particularly in systems exhibiting longer lifetimes.

In summary, by tuning the kinetic balance between the gelation and sol transition pathways, the lifetime of the transient hydrogel can be programmed over a broad timescale, ranging from an hour to three months. In terms of the energy landscape, mixing two polymers results in a transient thermodynamic state, in which the two polymers form hydrogel networks via coordination crosslinking at the termini of the precursors (Fig. 4). This state is dissipated through enzymatic dephosphorylation, which proceeds via de-crosslinking and yields a sol transition. The transient gel state persisted as a kinetically trapped state, facilitated by fast crosslinking and slow de-crosslinking pathways.

3.3. Programmed release of phosphate ester tagged payload

We performed model drug loading and release experiments using FDP (Fig. 3B) as the model payload (Fig. 5A). First, FDP was encapsulated in a hydrogel without ALPs. Then, the HEPES buffer (100 mM, pH 7.4) was added to the top of the hydrogel, and the release of payload into the supernatant was quantified via fluorescence spectroscopy. More than 80% of the loaded FDPs were retained in the hydrogel after three days (Fig. 5B). In contrast, when fluorescein without phosphate esters was used as a control, significant leakage from the hydrogel was observed within one day. These results indicate that compounds containing phosphate esters could be sufficiently incorporated into the hydrogel network. We then investigated whether transient hydrogels encapsulating ALPs could facilitate the release of FDPs via an autonomous sol transition. The release of FDPs was significantly accelerated by encapsulating ALPs within the hydrogel, indicating that ALP-catalyzed dephosphorylation eliminated the phosphate ester from FDP and allowed fluorophores to escape from the networks, accompanied by network degradation (Fig. 5B). The payload release rate tended to increase with increasing concentrations of ALPs encapsulated in the hydrogel, indicating the capability of the system for programmable and sustained payload release (Fig. 5C). We further demonstrated the programmed protein release using EGFP with E4pY tag at *C*-terminus (EGFP-Pi) as a model (Fig. 5A and Supporting information 12). When EGFP-Pi was encapsulated in the hydrogel without ALPs, almost all loaded proteins were retained in the hydrogel, while EGFP without tag leaked completely (Fig. 5D); the leakage of EGFP-Pi and EGFP were 1.2 $\pm$ 0.1% and 116 $\pm$ 9%, respectively after six days. The release of EGFP-Pi was accelerated by encapsulating ALPs within the hydrogel; 25 $\pm$ 8.1% of EGFPs was released after six days. The results demonstrate the universal ability of the hydrogel to perform programmable retention and release of payloads with a phosphate ester. This offers the possibility of loading various phosphorylated compounds, such as drugs, proteins, and cells, into hydrogels via phosphate ester tagging. It should be mentioned that numerous phosphate-esterified prodrugs have been reported [41].

3.4. Biocompatibility

Finally, the biocompatibility of the hydrogel was investigated using MDA-MB-231 cells. Prior to the cell experiments, hydrogel formation

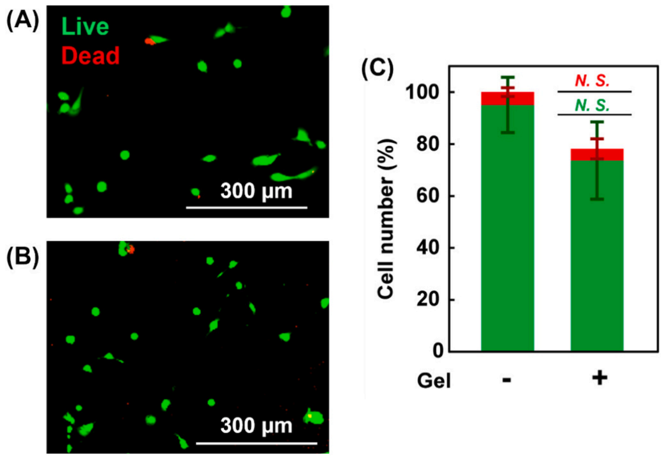

Fig. 6. Representative image of a live/dead stain (A) with and (B) without the hydrogel on cells. The polymer concentration was 120 g L^{-1}. (C) Cell number after 24 h incubation normalized by cells without the hydrogel. Cell population of live and dead cells are shown as green and red (n = 3). (For interpretation of the references to colour in this figure legend, the reader is referred to the web version of this article.)

was examined using cell culture media. Hydrogel formation was confirmed in the cell culture media when the polymer concentration was higher than 90 g L^{-1} (Supporting Information 13). The hydrogel was then formed on the cells and incubated for 24 h. Cell viability was assessed by live/dead staining using calcein-acetoxymethylester (calcein-AM) and ethdium homodeimer-1 (Fig. 6A and B). The results of the live-dead assay showed high cell viability after treatment, indicating the biocompatibility of the hydrogel (Fig. 6C).

4. Conclusion

In this study, we developed a transient and injectable hydrogel with a programmable lifetime by introducing closed functional loops, specifically gelation and sol transition pathways, within the system. The gel emerged in a transient thermodynamic state, which was dissipated by the encapsulated enzymes under out-of-equilibrium conditions. The transient gel state persisted because of the kinetic imbalance between the fast gelation and slow sol transition pathways. By tuning the kinetic balance of these pathways, the lifetime of the transient hydrogel was programmed in across a broad timescale, from within an hour to three months. The capability of the hydrogel to program payload release induced by sol transition was also validated by using phosphate ester-tagged small molecules and proteins as models. The unique properties of the present system are expected to have applications in drug delivery systems tailored to patient needs and objectives, as well as in scaffold materials for tissue engineering. The obtained results provide a foundation for engineering hydrogels that can dynamically regulate biological processes, and offers a strategy for the development of materials with autonomous, adaptive, and programmable functions that are far from equilibrium.

Declaration of AI technologies

No AI tool was used in the preparation of this manuscript.

CRediT authorship contribution statement

Ryo Sekiya: Writing – review & editing, Writing – original draft, Visualization, Validation, Investigation, Formal analysis, Data curation. **Masahiko Nakamoto:** Writing – review & editing, Writing – original draft, Supervision, Conceptualization. **Shunsuke Kato:** Writing – review & editing, Investigation, Formal analysis. **Takashi Hayashi:** Writing – review & editing. **Michiya Matsusaki:** Writing – review & editing, Supervision.

Funding sources

This work was supported by JSPS KAKENHI (JP24H01137 "Bottom-up Biotech") and JST FOREST (JPMJFR232E). This work was supported in part by JSPS KAKENHI (JP24K21106, JP22H05141 and JP22H05131).

Appendix A. Supplementary data

Supplementary data to this article can be found online at https://doi.org/10.1016/j.jconrel.2026.114867.

Data availability

Data will be made available on request.

References

[1] J.L. Drury, D.J. Mooney, Hydrogels for tissue engineering: scaffold design variables and applications, Biomaterials 24 (2003) 4337–4351.
[2] H. Fan, J.P. Gong, Fabrication of bioinspired hydrogels: challenges and opportunities, Macromolecules 53 (2020) 2769–2782.
[3] W. Wu, H. Chen, F. Shan, J. Zhou, X. Sun, L. Zhang, T. Gong, A novel doxorubicin-loaded in situ forming gel based high concentration of phospholipid for intratumoral drug delivery, Mol. Pharm. 11 (2014) 3378–3385.
[4] M. Shibayama, Universality and specificity of polymer gels viewed by scattering methods, Bull. Chem. Soc. Jpn. 79 (2006) 1799–1819.
[5] T. Sakai, T. Matsunaga, Y. Yamamoto, C. Ito, R. Yoshida, S. Suzuki, N. Sasaki, M. Shibayama, U. Chung, Design and fabrication of a high-strength hydrogel with ideally homogeneous network structure from tetrahedron-like macromonomers, Macromolecules 41 (2008) 5379–5384.
[6] T. Matsunaga, T. Sakai, Y. Akagi, U. Chung, M. Shibayama, SANS and SLS studies on tetra-arm PEG gels in as-prepared and swollen states, Macromolecules 42 (2009) 6245–6252.
[7] T. Matsunaga, T. Sakai, Y. Akagi, U. Chung, M. Shibayama, Structure characterization of tetra-PEG gel by small-angle neutron scattering, Macromolecules 42 (2009) 1344–1351.
[8] C. Norioka, K. Okita, M. Mukada, A. Kawamura, T. Miyata, Biomolecularly stimuli-responsive tetra-poly (ethylene glycol) that undergoes sol–gel transition in response to a target biomolecule, Polym. Chem. 8 (2017) 6378–6385.
[9] N. Yamaguchi, L. Zhang, B.-S. Chae, C.S. Palla, E.M. Furst, K.L. Kiick, Growth factor mediated assembly of cell receptor-responsive hydrogels, J. Am. Chem. Soc. 129 (2007) 3040–3041.
[10] L. Zhang, E.M. Furst, K.L. Kiick, Manipulation of hydrogel assembly and growth factor delivery via the use of peptide–polysaccharide interactions, J. Control. Release 114 (2006) 130–142.
[11] M. Ohira, T. Katashima, M. Naito, D. Aoki, Y. Yoshikawa, H. Iwase, S. Takata, K. Miyata, U. Chung, T. Sakai, M. Shibayama, Star-polymer–DNA gels showing highly predictable and tunable mechanical responses, X. Li, Adv. Mater. 34 (2022) 2108818.
[12] X. Bao, X. Si, X. Ding, L. Duan, C. Xiao, pH-responsive hydrogels based on the self-assembly of short polypeptides for controlled release of peptide and protein drugs, J. Polym. Res. 26 (2019) 278.
[13] M. Matsusaki, R. Amekawa, M. Matsumoto, Y. Tanaka, A. Kubota, K. Nishida, M. Akashi, Physical and specific crosslinking of collagen fibersby supramolecular nanogelators, Adv. Mater. 23 (2011) 2957.
[14] Z. Cimen, S. Babadag, S. Odabas, S. Altuntas, G. Demirel, G.B. Demirel, Injectable and self-healable pH-responsive gelatin–PEG/Laponite hybrid hydrogels as long-acting implants for local cancer treatment, ACS Appl. Polym. Mater. 3 (2021) 3504–3518.
[15] H. Deng, A. Dong, J. Song, X. Chen, Injectable thermosensitive hydrogel systems based on functional PEG/PCL block polymer for local drug delivery, J. Control. Release 297 (2019) 60–70.
[16] L.M. Coluccio, I. Myosin, Myosins, Proteins and Cell Regulation, 7, Springer, Dordrecht, 2008, pp. 95–124.
[17] G. Matsumoto, K. Wada, M. Okuno, M. Kurosawa, N. Nukina, Serine 403 phosphorylation of p62/SQSTM1 regulates selective autophagic clearance of ubiquitinated proteins, Mol. Cell 44 (2011) 279–289.
[18] K. Das, L. Gabrielli, L.J. Prins, Chemically fueled self-assembly in biology and chemistry, Angew. Chem. Int. Ed. 60 (2021) 20120–20143.
[19] J. Boekhoven, W.E. Hendriksen, G.J.M. Koper, R. Eelkema, J.H. Van Esch, Transient assembly of active materials fueled by a chemical reaction, Science 349 (2015) 1075–1079.
[20] S.M. Poprawa, M. Stasi, B.A.K. Kriebisch, M. Wenisch, J. Sastre, J. Boekhoven, Active droplets through enzyme-free, dynamic phosphorylation, Nat. Commun. 15 (2024) 4204.

[21] R. Yoshida, T. Takahashi, T. Yamaguchi, H. Ichijo, Self-oscillating gels, J. Am. Chem. Soc. 118 (1996) 5134–5135.
[22] M. Onoda, T. Ueki, R. Tamate, M. Shibayama, R. Yoshida, Amoeba-like self-oscillating polymeric fluids with autonomous sol-gel transition, Nat. Commun. 8 (2017) 15862.
[23] Y.S. Kim, R. Tamate, A.M. Akimoto, R., Yoshida recent developments in self-oscillating polymeric systems as smart materials: from polymers to bulk hydrogels, Mater. Horiz. 4 (2017) 38–54.
[24] R. Baretta, M. Frasconi, Electrically powered dissipative hydrogel networks reveal transient stiffness properties for out-of-equilibrium operations, J. Am. Chem. Soc. 146 (2014) 7408–7418.
[25] S. Maiti, I. Fortunati, C. Ferrante, P. Scrimin, L.J. Prins, Dissipative self-assembly of vesicular nanoreactors, Nat. Chem. 8 (2016) 725–731.
[26] X. Hao, L. Chen, W. Sang, Q. Yan, Periodically self-pulsating microcapsule as programmed microseparator via ATP-regulated energy dissipation, Adv. Sci. 5 (2018) 1700591.
[27] A. Mishra, S. Dhiman, S.J. George, ATP-driven synthetic supramolecular assemblies: from ATP as a template to fuel, Angew. Chem. Int. Ed. 60 (2021) 2740–2756.
[28] S. Debnath, S. Roy, R.V. Ulijn, Peptide nanofibers with dynamic instability through nonequilibrium biocatalytic assembly, J. Am. Chem. Soc. 135 (2013) 16789–16792.
[29] S. Hamada, K. Yancey, G.Y. Pardo, M. Gan, M. Vanatta, D. An, Y. Hu, T.L. Derrien, R. Ruiz, P. Liu, J. Sabin, D. Luo, Dynamic DNA material with emergent locomotion behavior powered by artificial metabolism, Sci. Robot. 4 (2019) eaaw3512.
[30] Q. Liu, H. Li, B. Yu, Z. Meng, X. Zhang, J. Li, L. Zheng, DNA-based dissipative assembly toward nanoarchitectonics, Adv. Funct. Mater. 32 (2022) 2201196.
[31] M. Nakamoto, S. Kitano, M. Matsusaki, Biomacromolecule-fueled transient volume phase transition of a hydrogel, Angew. Chem. Int. Ed. 61 (2022) e202205125.
[32] Y.K. Hong, M. Nakamoto, M. Matsusaki, Engineering metabolic cycle-inspired hydrogels with enzyme-fueled programmable transient volume changes, J. Mater. Chem. B 11 (2023) 8136–8141.
[33] H. Jo, S. Selmani, Z. Guan, S. Sim, Sugar-fueled dissipative living materials, J. Am. Chem. Soc. 145 (2023) 1811–1817.
[34] E. Kinoshita, M. Takahashi, H. Takeda, M. Shiro, T. Koike, Recognition of phosphate monoester dianion by an alkoxide-bridged dinuclear zinc(II) complex, Dalton Trans. 8 (2004) 1189–1193.
[35] E. Kinoshita, E. Kinoshita-Kikuta, K. Takiyama, T. Koike, Phosphate-binding tag, a new tool to visualize phosphorylated proteins, Mol. Cell. Proteomics 5 (2006) 749.
[36] E. Kinoshita, A. Yamada, H. Takeda, E. Kinoshita-Kikuta, T. Koike, Novel immobilized zinc(II) affinity chromatography for phosphopeptides and phosphorylated proteins, J. Sep. Sci. 28 (2005) 155.
[37] G. Stojkov, Z. Niyazov, F. Picchioni, R.K. Bose, Relationship between structure and rheology of hydrogels for various applications, Gels 7 (2021) 255.
[38] S. Gu, G. Cheng, T. Yang, X. Ren, G. Gao, Mechanical and rheological behavior of hybrid cross-linked polyacrylamide/cationic micelle hydrogels, Macromol. Mater. Eng. 302 (2017) 1700402.
[39] Tengjiao Zhu, Hufei Wang, Zehao Jing, Daoyang Fan, Zhongjun Liu, Xing Wang, Yun Tian, High efficacy of tetra-PEG hydrogel sealants for sutureless dural closure, Bioact. Mater. 8 (2022) 12.
[40] W. Chen, C. Wang, W. Liu, B. Zhao, Z. Zeng, F. Long, C. Wang, S. Li, N. Lin, J. Zhou, A matrix-metalloproteinase-responsive hydrogel system for modulating the immune microenvironment in myocardial infarction, Adv. Mater. 35 (2023) 2209041.
[41] H. Yu, H. Yang, E. Shi, W. Tang, Development and clinical application of phosphorus-containing drugs, Med. Drug Discov. 8 (2020) 10006.